

SYNTHESIS AND OPTICAL CHARACTERIZATION OF BUILDING-BLOCK PLASMONIC GOLD NANOSTRUCTURES

OANH THI TU NGUYEN, CHI HA LE, LONG DUY PHAM,
HIEU SY NGUYEN AND CHUNG VU HOANG[†]

*Institute of Materials Science, Vietnam Academy of Science and Technology,
18 Hoang Quoc Viet street, Cau Giay district, Hanoi, Vietnam*

[†]*E-mail:* chunghv@ims.vast.ac.vn

Received 07 April 2017

Accepted for publication 14 June 2017

Published 30 June 2017

Abstract. *Plasmonics, the field involves manipulating light at the nanoscale, has been being an emergent research field worldwide. Synthesizing the plasmonic gold nanostructures with controlled morphology and desired optical properties is of special importance towards specific applications in the field. Here, we report the chemical synthesis and the optical properties of various plasmonic Au nanostructures, namely Au nanoparticles (AuNPs), Au nanorods (AuNRs) and random Au nano-islands (AuNI) that are the building blocks for plasmonic research. The results show that the AuNPs exhibited a single plasmonic resonance, the AuNRs displayed two identical and separated modes of the resonance, and the random Au nano-islands presented a very broad resonance. Specifically, tailoring the anisotropy of the Au nanorods enabled extending their resonant frequencies from the visible to the near infrared region, which is in accordance with the finite different time domain simulations.*

Keywords: Plasmonics, chemical synthesis, optical property, nanoparticles, nanorods, random nano-islands.

Classification numbers: 73.20.Mf, 81.10.Dn, 81.07.Bc, 42.25.Dd, 78.40.q.

I. INTRODUCTION

The interaction of light with the metal nanostructures opens up plasmonics, an emergent field which is multidisciplinary and involves many different subjects such as physics, chemistry, materials science, biochemistry, medicine and beyond [1–5]. In plasmonics, impinging of light on the metal nanostructures induces the coherent oscillation of the free electron gas at the metal surface [6–8]. Specifically, the plasmonic nanostructures show their extraordinarily large optical cross-section that confines the incident light (electromagnetic radiation) into a small volume whose dimensions are much smaller than the wavelength of the incident light [9]. This offers the possibility to enhance the electromagnetic field and to promote the internal photoemission of the hot-electrons from the metal surface [3–6, 10, 11]. Therefore, there has been an increasing interest in plasmonic applications in the fields of solar energy conversion, novel electronics devices, new medical treatment approaches, and green chemistry.

Fabrication of the nanostructures that are the building-blocks for plasmonic systems is vital for realizing their future applications. In addition to the physical approach, the chemical one is a powerful way as it follows the bottom-up route and the cost-effective strategy. Particularly, the chemical approach can effectively control the size, shape and the correspondent optical properties of the nanostructures, which is apparently of special importance in this field. In this paper, we report on the chemical synthesis and optical properties of various plasmonic nanostructures, namely gold nanoparticles (AuNPs), gold nanorods (AuNRs), and the random gold nano-islands (AuNI).

II. EXPERIMENTAL

Materials

Hexadecyltrimethyl ammonium bromide (CTAB) (98%, Sigma-Aldrich), benzyldimethyl-hexadecyl ammonium chloride hydrate (BDAC) (97%, Acros), sodium borohydride (99%, Acros) silver nitrate (99.9%, Fisher), L-ascorbic acid (99%, Sigma-Aldrich), gold(III) chloride trihydrate (49% Au basis, Sigma-Aldrich), sodium citrate dihydrate (99%, Aldrich), (3-aminopropyl) triethoxysilane (APTES, 99% Aldrich), and ethanol (HPLC, Sigma-Aldrich), acetone (Fisher) were used as purchased. Milli-Q water ($18 \text{ M}\Omega\text{cm}^{-1}$) was used in all aqueous solutions. Corning[®] plain microscope slides (Aldrich) were cut into pieces of chosen sizes. The glass pieces were cleaned consecutively in Decon 90 (Fisher) of 5% in vol., distilled water, ethanol, acetone, and double distilled water for 10 minutes each in an ultrasonic cleaner. The cleaned glass pieces were dried in air before use.

Synthesis of spherical gold nanoparticles

In our experiments, we synthesized spherical gold nanoparticles (AuNPs) by citrate reduction method [12]. Gold nanoparticle solutions are prepared by chemical reduction of gold (III) chloride trihydrate as a gold precursor and sodium citrate dihydrate as a reducing agent. The growth process of AuNPs was controlled by reactant concentrations and temperature. First, add 10 ml of 38.8 mM sodium citrate solution into 100 ml of boiling 1mM HAuCl_4 solution that was vigorously stirred. Then, keep the obtained solution boiling for 15 minutes. The color of solution changed from yellow to dark blue and finally red color. After that the solution was cooled down and stored in the fridge.

Synthesis of gold nanorods

The gold nanorod solutions were prepared following the procedure published by Nikoobakht and El-Sayed [13]. The gold nanoparticle seed solution was prepared before growing gold nanorods. The seed solution was made by adding 0.6 ml of ice-cold 0.010 M NaBH₄ into the vigorously stirred solution of 5 ml of 0.20 M CTAB solution and 5 ml of 0.00050 M HAuCl₄. Keep stirring for 2 minutes. The obtained seed solution was kept at 25°C before use. As for the growth of gold nanorods with plasmon band less than 850 nm: adding 5 ml of 1 mM HAuCl₄ into 5 ml of 0.2M CTAB solutions containing 50 or 100 or 200 μ l of 0.0040 M AgNO₃ solution at 25°C. After gentle mixing of each solution, adding 70 μ l of 0.0788 M ascorbic acid, the color of the growth solution changed from dark yellow to colorless. Finally, adding 12 μ l of the seed solution to the growth solution at 27-30°C. The color of the solution gradually changed within 10-20 minutes.

Synthesis of gold nano-islands

The gold nano-island films were grown from gold spherical nanoparticles as seeds that were immobilized by APTES onto glass substrates. First, immerse glass pieces in solution of APTES of 10 wt% to produce the APTES-functionalized glass substrates. Next, immerse the APTES-functionalized glass substrates in the gold nanoparticles solution for 30 minutes. As a result, the AuNPs were attached onto glass substrates via amino group of APTES as seen in Fig. 1. After rinsing with double distilled water, the AuNPs films were dried in air. Finally, the gold islands evolved from those immobilized gold nanoparticles when the immobilized gold nanoparticle film was submerged in a solution of 0.3 mM HAuCl₄ and 0.4 mM NH₂OH on an orbital shaker at room temperature. As the growth time was lengthened, the gold nanostructures increased in size and the film color changed from red at the beginning to grey, then dark blue, and lastly to shining gold. The resulting Au nano-island films were taken out at different growth times (15 minutes, 35 minutes and 45 minutes), rinsed by double distilled water and dried in air.

Sample characterization

The morphology of gold nanostructures was investigated by using field emission scanning electron microscopy (FE-SEM, Hitachi S-4800) and transmission electron microscopy (TEM, JEOL JEM1010). The Ultraviolet-visible (UV-vis) absorption spectra were performed by using a Jasco V-670 UV-VIS spectrometer.

III. RESULTS AND DISCUSSION

Synthesis and optical property of gold nanoparticles

Figure 1 shows a typical transmission electron microscope (TEM) image of the Au nanoparticles (AuNPs) prepared by the citrate reduction method. Gaussian fitted curve of AuNPs diameter distribution presented in Fig. 1b indicates that AuNPs had an average diameter of 14 ± 2 nm (the error bar is the standard deviation of the fit). The particle size obtained in this work is similar to that of the data reported by Turkevich [12]. The optical absorption of the AuNPs in the aqueous solution is shown in Fig. 1c. The absorption spectrum of the AuNPs displays a plasmonic resonance peak located at approximately 550 nm. It is worth noticing that for the wavelength shorter than 520 nm, the bulk Au has an interband absorption that induces a strong absorption in the Au materials [14]. The asymmetric absorption tail in the high energy side of the spectrum presented in Fig. 1c reflects this fact. As presented in Fig. 1a, the AuNPs seem

to be paired together. However, this was due to the process of transferring the AuNPs from the solution to the copper grid for the TEM measurements. In the aqueous solution, the AuNPs were well-dispersed as there was no additional resonance peak appeared in Fig. 1c.

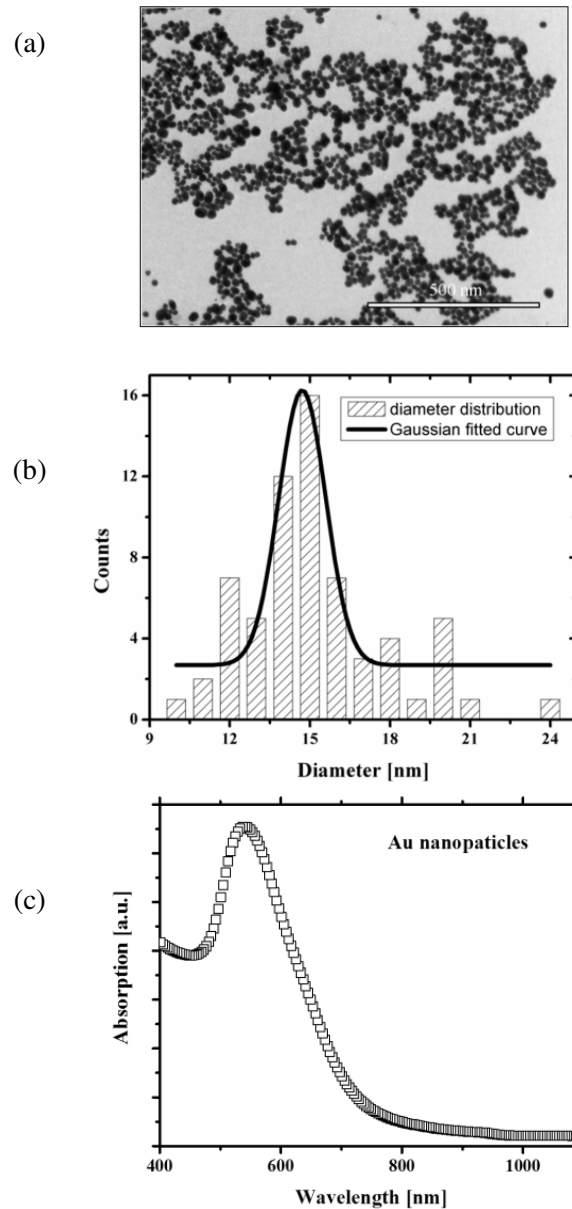


Fig. 1. (a) Transmission electron microscope (TEM) image of the Au nanoparticles. (b) Diameter distribution of the Au nanoparticles presented in (a). (c) Optical absorption of the Au nanoparticles, measured in the aqueous solution environment.

Synthesis and optical property of gold nanorods

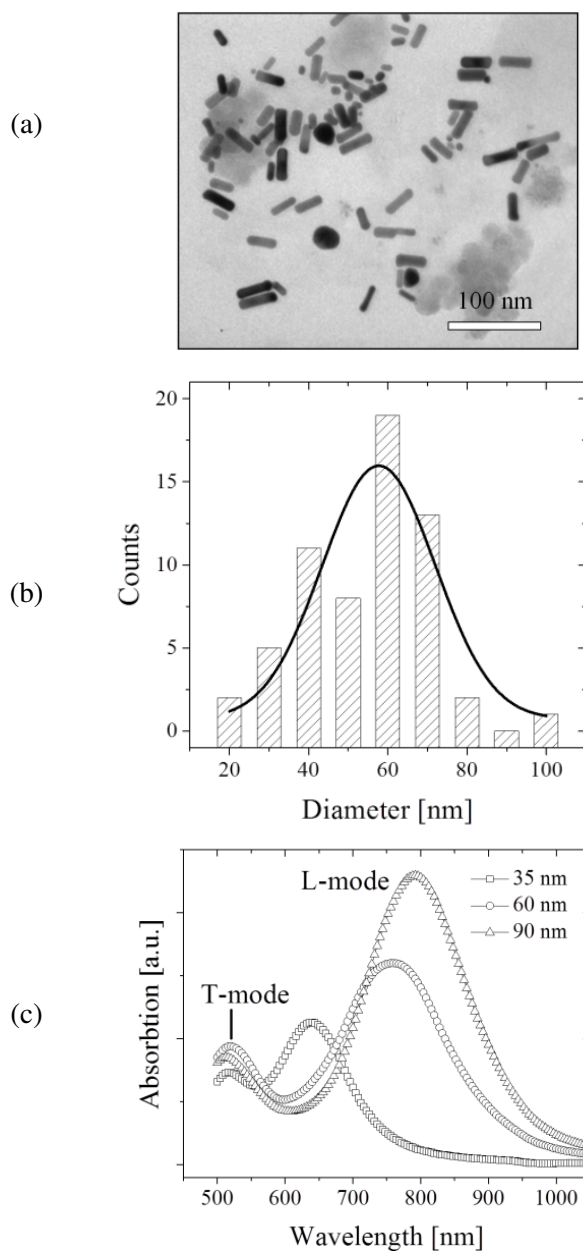


Fig. 2. Morphological and optical characterization of the Au nanorods. (a) Transmission electron microscope (TEM) image of a kind of Au nanorods. (b) The distribution in length of the nanorods presented in (a). (c) Optical absorption of the gold nanorods with different average lengths, ranging from 35 nm, 60 nm and 90 nm, which were measured at the same growth time.

Figure 2 shows morphological and optical characterization of the AuNRs. Fig. 2a presents a typical TEM image of the AuNRs. From the TEM image, we can see that most of products are AuNRs of similar sizes, but there are still some unwanted gold nanoparticles of different sizes. The particle distribution reveals that the AuNRs has the average length of approximately 60 nm and the width is about 15 nm (not shown). The Gaussian distribution curve is rather broad, having the full-width at half of maximum of about 30 nm. Fig. 2c presents the optical absorption spectra of the AuNRs of different average lengths. It is seen that compared to the absorption of the Au nanoparticles, the spectra of the 35 nm, 60 nm and 90 nm Au nanorods displayed two distinct resonance peaks. There was one common peak at approximately 515 nm and the other peak was shifted to the lower energy side if the rod was longer. Specifically, this peak shifted from 640 nm to 780 nm when the length of the rod increased from 35 nm to 90 nm. In addition, the absorption intensity of both peaks increased when the rod length grew from 35 nm to 90 nm.

The morphology of the Au nanorods depends on various experimental conditions such as the reactant concentrations, temperature, pH, additives and surfactants. For example, the molar ratio of AgNO_3 is one of the critical parameters for the length of the nanorods. In our experiment, the increase in amount of AgNO_3 solution from 50 μL to 100 μL and 200 μL caused the length of gold nanorods (AuNRs) to increase from 35 nm to 90 nm whose optical absorption spectra are presented in Fig. 2c.

The relationship between the absorption intensity and the shape of the nanorods was explained by Gans theory [15]. The plasmon absorption is a function of the volume of the nanorods, dielectric constants of the surrounding media and nanorod materials, and the aspect ratio of the nanorods:

$$\sigma_{\text{abs}} = \frac{2\pi V}{3\lambda} \epsilon_m^{3/2} \sum_{j=1}^3 \frac{(1/P_j^2) \epsilon_2}{[\epsilon_1 + \epsilon_m P_j / (1 - P_j)]^2 + \epsilon_2^2}, \quad (1)$$

where V is the volume of the nanorod; ϵ_m , $\epsilon = \epsilon_1 + \epsilon_2$, are the dielectric constants of the medium and the real and imaginary part of the metal, respectively; P_j is the depolarization factor that accounts for the aspect ratio of the nanorod. Specifically, it is:

$$P_A = \left(\frac{1 - e^2}{e^2} \right) \left\{ \frac{1}{2e} \ln \left(\frac{1 + e}{1 - e} \right) - 1 \right\}, \quad (2)$$

where P_A is the depolarization factor in the longitudinal direction of the nanorod; e is the factor that is determined by the aspect ratio of the nanorods and $e = \sqrt{1 - 1/r}$ where r is the aspect ratio along this direction.

Figure 3 presents the evolution of the plasmonic absorption of the AuNPs in the solution which had been used for the synthesis of the nanorods. Fig. 3a shows the spectral development of the two distinct plasmonic peaks with time. The 0-min curve shows the spectrum of the AuNPs as just prepared. After 70 min, we obtained a significant increase of the plasmon intensity without any shift of the plasmon frequency. This effect is fairly well explained by looking at Eq. (1). Since the surrounding (ϵ_m) and metal (ϵ_1, ϵ_2) dielectric functions stay the same, the absorption intensity is mainly affected by the volume of the Au nanorods (V) and the aspect ratio (r), in which σ_{abs} is directly proportional to V . However, the change of the shape and volume of the nanorods also lead to the shift of the plasmon frequencies, as reported in the literature [16]. Therefore, the main reason to be attributed for the monotonic increase of the σ_{abs} is the increase of the density of

the nanorods versus time. Figure 3b shows the monotonic rise in σ_{abs} along the longitudinal and transverse directions of the nanorods. It is seen that the L-mode presents a slope with one-order of magnitude higher than that of the T-mode.

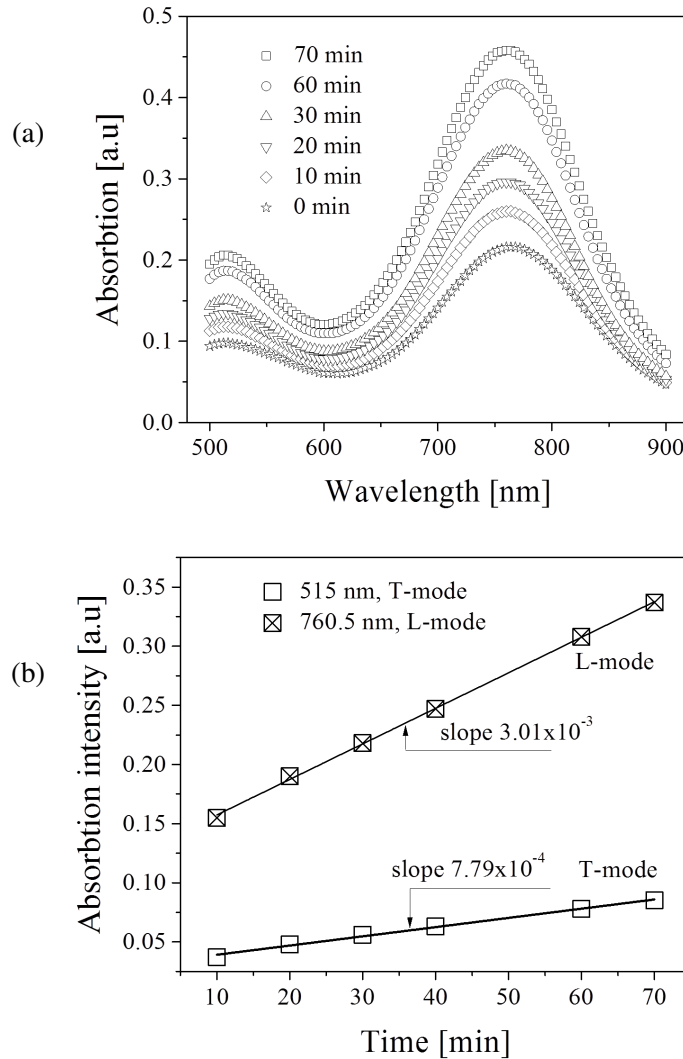


Fig. 3. Time evolution of the plasmonic absorption of the AuNPs. (a) Evolution of the plasmonic absorption of the AuNPs in the aqueous solution, measured every 10 minutes. The black curve (0 min) presents the absorption of the AuNPs as just prepared. (b) The evolution of the two distinct plasmon peaks, noted as transverse mode (T-mode) and longitudinal mode (L-mode).

The plasmon frequency of the nanorods depends on the size, shape and dielectric constants of the metal and surrounding medium [16]. In the visible and near infrared range, the analytical solution for this relationship is rather complex as it is close to the interband and intra band transitions

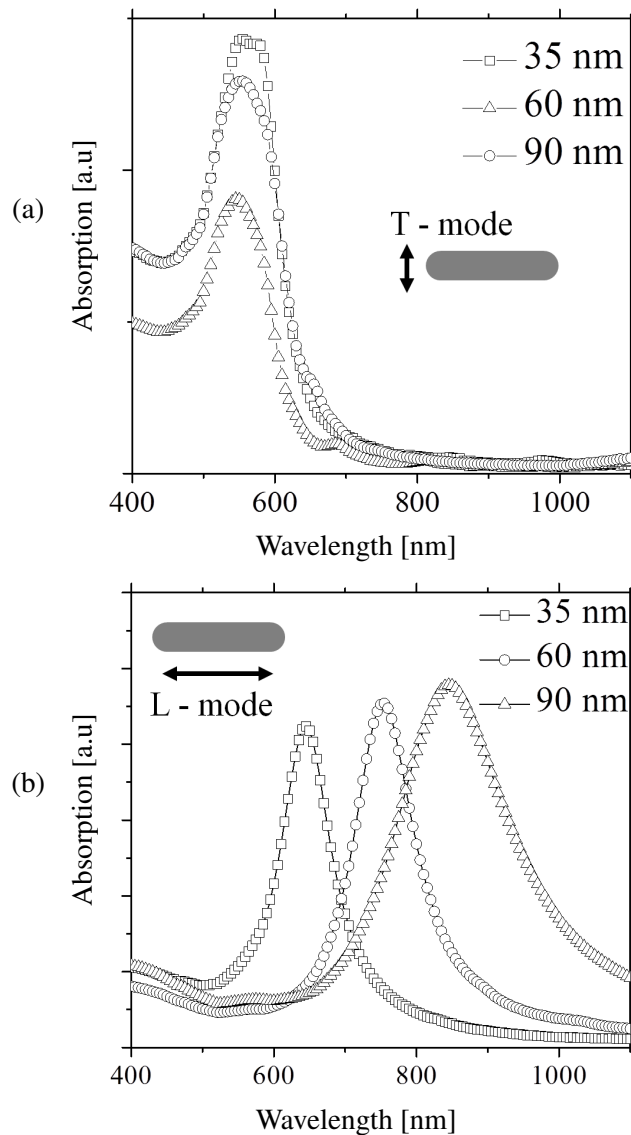


Fig. 4. Finite different time domain (FDTD) simulations of the optical property of the Au nanorods. (a) and (b) are the simulated absorption spectra of the gold nanorods under the excitations that are perpendicular and parallel to the longitudinal direction of the gold nanorods, respectively.

of the Au metal. Therefore, the origin of the peaks obtained in the absorption of the Au nanorods can be understood and confirmed by the numerical simulation only. Here, the finite different time domain (FDTD) simulation was employed for the investigation. The simulated scattering spectra of the nanorods with different lengths of 35 nm, 60 nm and 90 nm under two excitation conditions are presented in Fig. 4.

As seen in Fig. 4, if the excitation is perpendicular to the longitudinal direction of the nanorods (T-mode), there is only one resonance peak at 540 nm. However, under the longitudinal excitation condition (L-mode), we clearly see that the plasmon resonance is shifted as the rods are longer. Since the spectra of the Au nanorods presented in Fig. 2c were measured under the non-polarized excitation, two plasmon modes associated to the transverse and longitudinal oscillation of the free electrons in the nanorods could be seen at the same time.

Synthesis and optical property of self-assembled random gold nano-islands

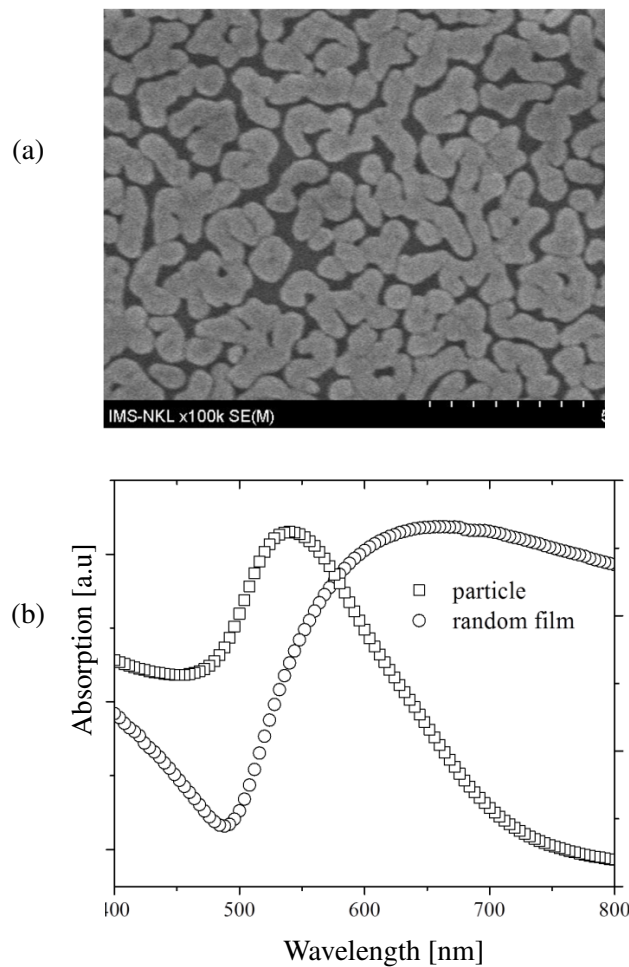


Fig. 5. (a) Field-emission scanning electron microscope (FESEM) images of a typical random Au nano-islands grown on the APTES-functionalized glass substrate with growth time of 35 minutes. (b) Optical absorption spectrum of the random Au nano-islands. The absorption of the Au nanoparticles is also shown in (b) for the comparison.

We adopted the method of growing the self-assembled random Au nano-islands from Enders *et al.* [17]. As seen in Fig. 5, the Au film consisted of random Au nano-islands that were

separated by nanogaps. The shape of the Au islands was very complex and the gold coverage was approximately 80% of the total glass surface after 35 min of growth. The optical extinction spectrum of this sample is presented in Fig. 5b. The spectrum of the Au nanoparticles is shown for comparison. As seen in Fig. 5b, the spectrum of the random Au nano-islands film was very broad, ranging from the visible to the near infrared frequencies. A common strong absorption below 500 nm is assigned to the interband absorption of the bulk Au materials. With the given nanogap architecture, this random Au nano-islands is highly suitable for the application to the surface-enhanced spectroscopies [11].

IV. CONCLUSIONS

We have presented the synthesis as well as the optical characterization of the plasmonic building-blocks that are Au nanoparticles, nanorods and random nano-islands. The plasmon resonance of the AuNPs was composed of a single plasmonic peak. Meanwhile, the Au nanorods exhibited a co-existence of two modes associated to the oscillation of the free electrons in the longitudinal and transverse directions of the Au rods. The Au nanorods offer the possibility to tune the plasmon resonance in a very broad range, from visible to the near infrared frequencies by tailoring the shape of the Au nanorods. The random Au nano-island film showed a very complex structure consisting of the separate islands with the nanogaps in between. The random Au nano-islands exhibited a very broad resonance range, superimposed by many separate resonators. This work might serve as a reference for the chemical synthesis of the plasmonic building-blocks and the fundamental understanding of their plasmonic resonance.

ACKNOWLEDGMENT

This research is funded by Vietnam National Foundation for Science and Technology Development (NAFOSTED) under grant number “103.02-2013.71”. The authors thank the fruitful discussions with Prof. Tadaaki Nagao and Dr. Thang D. Dao, NIMS, Tsukuba.

REFERENCES

- [1] S. Kawata, Y. Inouye, P. Verma, *Nat. Photon.* **3** (2009) 388–394.
- [2] T. S. Bui, T. D. Dao, L. H. Dang, L. D. Vu, A. Ohi, T. Nabatame, Y. Lee, T. Nagao, C. V. Hoang, *Sci. Rep.* **6** (2016) 32123.
- [3] E. W. McFarland, J. Tang, *Nature* **421** (2003) 616–618.
- [4] M. T. Sheldon, J. van de Groep, A. M. Brown, A. Polman, H. A. Atwater, *Science* **346** (2014) 828–831.
- [5] M. W. Knight, H. Sobhani, P. Nordlander, N. J. Halas, *Science* **332** (2011) 702–704.
- [6] M. L. Brongersma, N. J. Halas, P. Nordlander, *Nat. Nanotechnol.* **10** (2015) 25–34.
- [7] C. Sönnichsen, T. Franzl, T. Wilk, G. von Plessen, J. Feldmann, O. Wilson, P. Mulvaney, *Phys. Rev. Lett.* **88** (2002) 077402.
- [8] P. Mühlischlegel, H.-J. Eisler, O. J. F. Martin, B. Hecht, D. W. Pohl, *Science* **308** (2005) 1607–1607.
- [9] W. L. Barnes, A. Dereux, T. W. Ebbesen, *Nature* **424** (2003) 824–830.
- [10] F. Benz, M. K. Schmidt, A. Dreismann, R. Chikkaraddy, Y. Zhang, A. Demetriadou, C. Carnegie, H. Ohadi, B. de Nijs, R. Esteban, J. Aizpurua, J. J. Baumberg, *Science* **354** (2016) 726–729.
- [11] C. V. Hoang, M. Oyama, O. Saito, M. Aono Tadaaki Nagao, *Sci. Rep.* **3** (2013) 1175.
- [12] J. Turkevich, P. C. Stevenson & J. Hillier, *Discuss. Faraday. Soc.* **11** (1951) 55–75.
- [13] B. Nikoobakht, M. A. El-Sayed, *Chem. Mater.* **15** (2003) 1957–1962.
- [14] P. Johnson R. Christy *Phys. Rev. B* **6** (1972) 4730–4739.

- [15] J. Olson S Dominguez-Medina A Hoggard L-Y Wang W-S Chang S Link, *Chem. Soc. Rev.* **44** (2015) 40–57.
- [16] Novotny, *Phys. Rev. Lett.* **98** (2007) 266802.
- [17] D. Enders, T. Nagao, A. Pucci, T. Nakayama & M. Aono., *Phys. Chem. Chem. Phys.* **13** (2011) 4935–4941.